Toward Superhydrophobic and Durable Coatings: Effect of Needle vs Crater Surface Architecture

Brendan P. Dyett,[‡] Alex H. Wu,[‡] and Robert N. Lamb*,[‡]

School of Chemistry, University of Melbourne, Parkville, Victoria, 3010, Australia

Ⓢ Supporting Information

ABSTRACT: Practical application of sol–gel derived super-hydrophobic films is limited by the fragility of "needlelike" surface roughness. An efficient one step procedure is developed to prepare robust thin films with "craterlike" surface roughness from a methyltrimethoxysilane matrix and polymer sphere templates. The films could be readily spray coated to produce roughened surface textures, which are governed by template concentration and geometry. The effect of this on the wettability and robustness of thin films was examined in detail, revealing a rapid trade-off between the two characteristics due to variations in coating porosity.

KEYWORDS: crater, sol–gel, superhydrophobic, durable, fragile, spray
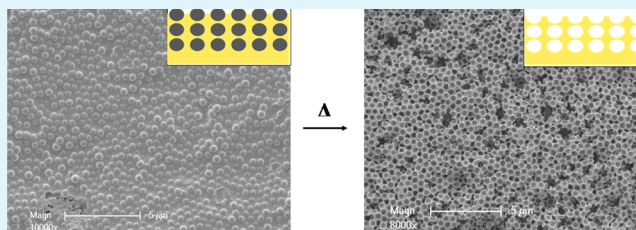
1. INTRODUCTION

The manifestation of low surface energy chemistry and surface roughness to yield superhydrophobic films (SHF) has ignited interest toward self-cleaning[1,2] and nonfouling surfaces.[3] Defined as water contact angles greater than 150° and rolling angles less than 5°, the superhydrophobic state is often understood with the Cassie–Baxter wetting model where, upon sufficient surface roughness, a solid–liquid interface is substantially replaced by solid–air interaction.[4] Facile fabrication of SHF is accessible through sol–gel synthesis;[5] however, practical application is hindered by the fragile nature of surface roughness employed.[6] The majority of SHF produced through sol–gel methods yield needlelike[7,8] surface roughness through the aggregation of nanoparticle clusters. This "needle" or "spike" geometry minimizes contact area, enhancing non-wetting behavior, yet it also results in high contact pressures upon load.[9] Consequently, the superhydrophobic nature of these films is vulnerable to mechanical damage diminishing surface roughness. Nakajima et al.[7] demonstrated employing craterlike roughness as a more durable alternative. Phase separation and subsequent thermal decomposition of an organic polymer dispersion from within silica matrix yielded thin films with voids akin to craters. Upon postfunctionalization with fluorosilanes, these films yielded surfaces with contact angles above 150° and pencil hardness above 4H. Despite demonstrating greatly increased abrasive resistance, this approach has been relatively under explored in literature, with only few examples utilizing crater roughness.[10−13] In this work, sol–gel preparation toward developing a one-step procedure toward robust superhydrophobic surfaces with template controlled crater roughness and intrinsic chemical phobicity is investigated.

2. EXPERIMENTAL SECTION

2.1. Materials. Methyltrimethoxysilane (95%, Sigma), methanol (AR, Chem-Supply), hydrochloric acid (37%, Scharlau), sodium dodecyl sulfate (AR, Sigma), hexadecane (99%, Sigma), ascorbic acid (Ajax), and hydrogen peroxide (30%, Chem-Supply) were used as received without further purification. Styrene (Sigma) was washed with dilute sodium hydroxide to remove inhibitor.

2.2. Preparation of Polymer Templates via Emulsion Synthesis. Emulsion polymerization was used to prepare polystyrene spheres 300−900 nm in diameter in accordance to the method previously described by Zhang et al.[14] This method describes the use of SDS as surfactant however cmc equivalents of CTAB can also be used. Polymer spheres with diameters 50−200 nm were prepared by miniemulsion following an adapted method previously described by Anderson et al.[15] Styrene (20 g) and hexadecane (0.8 g) were mixed before addition to sodium dodecyl sulfate (0.01−0.15 g) dissolved in Milli-Q water (80 mL). This mixture was dispersed by mechanical shear to yield an emulsion. Following emulsification the solution was purged by nitrogen gas before redox initiation using ascorbic acid (0.05 g) and hydrogen peroxide (0.10 mL). The reaction was held at 50 °C for 8 h.

2.3. Preparation of Coating Solution. Methyl trimethoxysilane (MTMS) (2.4 g, Sigma) was dispersed in methanol (50 mL) and Milli-Q water (5 mL) before subsequent addition of HCl (37%, 3 drops). This solution was reacted overnight before the addition of polymer spheres (varied to achieve desired weight percent). Silica nanoparticles can be utilized provide additional nanotexture. This mixture was sonicated (40 kHz, Unisonics) for 30 min before spraying coating (Scorpion HVLP gravity fed, 10 PSI) onto glass microscope slides. Coating slides were thermally treated to 350 °C for 1 h at a ramp of 1 °C/min.

2.4. Film Characterization. Surface chemistry was acquired using a VG ESCALAB220i-XL spectrometer (XPS) equipped with a

ACS Publications © 2014 American Chemical Society

9503

dx.doi.org/10.1021/am501900b | ACS Appl. Mater. Interfaces 2014, 6, 9503–9507

hemispherical analyzer. The incident radiation was monochromatic Al Kα X-rays (1486.6 eV) at 220 W (22 mA and 10 kV). Survey (wide) and high resolution (narrow) scans were taken at analyzer pass energies of 100 and 50 eV, respectively. Survey scans were carried out over 1200−0 eV binding energy range with 1.0 eV step size and 100 ms dwell time. Base pressure in the analysis chamber was below 7.0×10^{-9} mbar and during sample depth profile analysis 1.5×10^{-7} mbar. A low energy flood gun was used to compensate the surface charging effect. All data were processed using CasaXPS software, and the energy calibration was referenced to the C 1s peak at 284.7 eV. Surface and particle morphology was investigated using a Philips XL30 FESEM at 2.0 keV. Particle sizing was determined using a Malvern Zetasizer ZSP. The thermal decomposition of templates was determined using PerkinElmer Diamond TGA. The durability of films was characterized by pencil hardness in accordance to ASTM D3363-92a,[16] utilizing pencils softest to hardest (8B to 9H), nominal loading of 500 g, at angle of 45° over minimum distance of 6.5 mm. The hydrophobicity was characterized via static contact angles determined by Ramé-Hart goniometer (Model 100).

3. RESULTS AND DISCUSSION

3.1. Structural Templates. Spherical templates can be employed to reveal a craterlike surface upon removal.[17] The use of discrete templates offers several benefits in comparison to phase separation methods. The preparation of polymer sphere templates readily affords tunable surface structures in accordance to template size. The control of feature size may have profound impact toward biological repellence.[3] Moreover, discrete templates enable templating on multiple size regimes. Polystyrene spheres were chosen as templates owing to the relatively simple preparation and size control. To maximize control of surface structure the size dispersity (PDI) of the templates should be minimized. Size characterization for templates is summarized in Table 1. Example morphology is shown in Figure 1.

Table 1. Size Characterization Determined by DLS for Polymer Spheres Produced through Emulsion Synthesis

sample	size (nm)	PDI
A	530	0.060
B	417	0.019
C	670	0.022
D	230	0.002
E	100	0.011

3.2. "Crater−Structure" Films. The majority of sol−gel derived superhydrophobic films derive from the clustering of nanoparticles to form "needlelike" surface structures, illustrated in Figure 2. At the boundary of the film there is minimal material to withstand physical forces. Consequently, these particulate structures are readily abraded. Methods to resolve this issue is often focused on the chemistry[18,19] of binding agents such as polymers also present within the film, initially reported by Zhang et al.[5,20] This approach can be thwarted by difficulty managing the desired surface energy and preventing binding agents such as polymers drowning out surface roughness. Given that wetting behavior is routinely described through both chemical and geometric qualities and the longstanding challenges with chemical strategies, the exploration of more robust surface geometries such as crater structures presents a viable alternative to improve durability—regardless of the chemistry utilized. By employing craterlike roughness, the asperities are able to dissipate loads through increased solid surface area.[7] In addition, the use of a continuous glassy
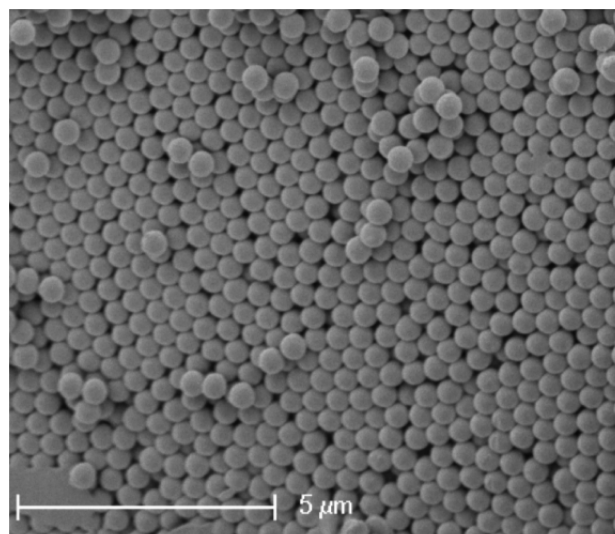

Figure 1. Example SEM micrograph of 500 nm polystyrene spheres.
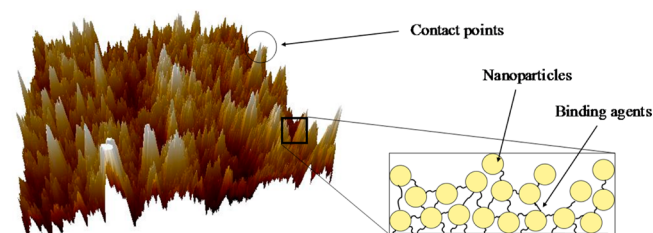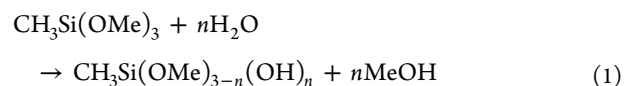

Figure 2. (left) Topological AFM image of conventional nanoparticle derived superhydrophobic films prepared in accordance with the work of Jones et al.[5] highlighting needlelike contact points of surface structures. (right) Schematic illustrating a magnified cross section of coating derived of nanoparticle clusters and binding agents.
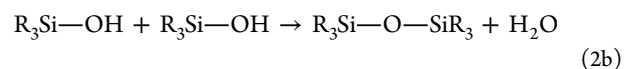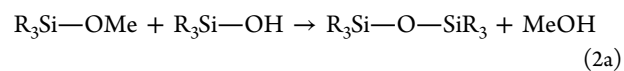
material further avoids durability issues of high filler content particle clusters.[21−23]

Craterlike films with varying feature sizes were developed from an MTMS based gel to which polymer sphere templates were embedded. The MTMS gel was formed through acid catalyzed polyhydrolysis and condensation reactions[24] (eq 1−2b) before thermal treatment to 350 °C which simultaneously hardens the siloxane matrix and decomposes polystyrene templates yielding roughened surface textures.

Hydrolysis

$$CH_3Si(OMe)_3 + nH_2O$$
$$\rightarrow CH_3Si(OMe)_{3-n}(OH)_n + nMeOH \quad (1)$$

Condensation

$$R_3Si\text{—}OMe + R_3Si\text{—}OH \rightarrow R_3Si\text{—}O\text{—}SiR_3 + MeOH \quad (2a)$$

$$R_3Si\text{—}OH + R_3Si\text{—}OH \rightarrow R_3Si\text{—}O\text{—}SiR_3 + H_2O \quad (2b)$$

Polymer spheres are conventionally allowed to self-assemble into close-packed colloidal crystal templates.[25] Upon self-assembly the close packed system is impregnated with a secondary solution which fills the octahedral and tetrahedral voids. The self-assembly process is slow and typically not achievable during spray coating procedures. Nonetheless a one-step spray coating with a volatile solvent still yielded consistent
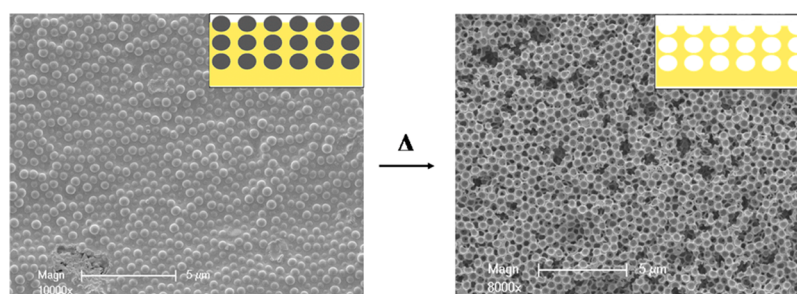
9504

dx.doi.org/10.1021/am501900b | ACS Appl. Mater. Interfaces 2014, 6, 9503−9507

Figure 3. SEM micrographs of craterlike films before (left) and after (right) temperature treatment at 350 °C. A schematic illustration is incorporated in the top right.
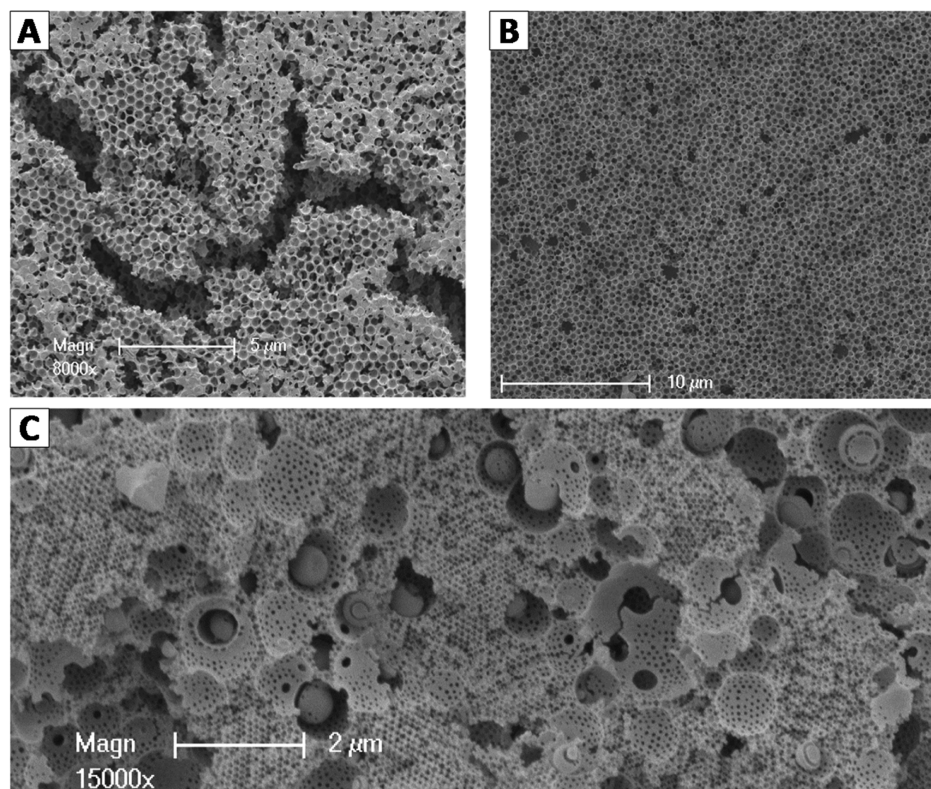

Figure 4. SEM micrographs of craterlike films prepared with (A) TEOS matrix, (B) MTMS with 417 nm template, and (C) with two templates, 100 and 1000 nm.

well dispersed films of templates engulfed within the MTMS gel, demonstrated in Figure 3. Spray coating yielding well dispersed films enhances the scale-up potential for this method. MTMS was used in favor of tetraethoxysilane (TEOS) to afford intrinsic hydrophobicity and reduce cracking (Figure 4a) through flexibility[26] and minimizing drying stress,[27−29] facilitating the development of crack-free surfaces across a broad range of single and multiple template sizes, demonstrated in Figure 4b and c. The packing on multiple scales (Figure 4c) was less ideal than single size systems; however, it has been reported this could be addressed through binary size relationship[30] and template surface chemistry.[31]

The water droplet contact angle is a reflection of both surface chemistry and surface roughness. XPS was used to investigate the surface chemistry of the films. From Table 2, it was inferred that surfactant and template residue (C, Na) is present after the thermal decomposition of templates. Upon washing, this residue is removed and contact angles were improved. The remaining carbon composition is attributed to methyl groups of

Table 2. XPS Survey Spectrum Data for Crater-Structures Generated Prior and after Washing with Milli-Q

element	position (eV)	atomic %	atomic % washed
O 1s	529.00	32.88	43.35
C 1s	285.00	42.54	21.44
Na 1s	1070.00	0.38	
Si 2p	100.00	24.20	35.21

MTMS based gel which provides an intrinsic hydrophobicity. The use of hydrophobic material removes complications of mechanical damage revealing hydrophilic groups.[6]

For expedience and uniformity with industry methods crater structure samples were further characterized by pencil hardness and contact angle during development. Previous reports using TEOS indicated that these surfaces should yield gouge pencil hardness between 4H and 6H.[7] Typical nanoparticle derived films[20,32] exhibit at contact angles above 160° however exhibit

very low pencil hardness, typically 8B. An array of results for crater films prepared is summarized in Figures 5 and 6.
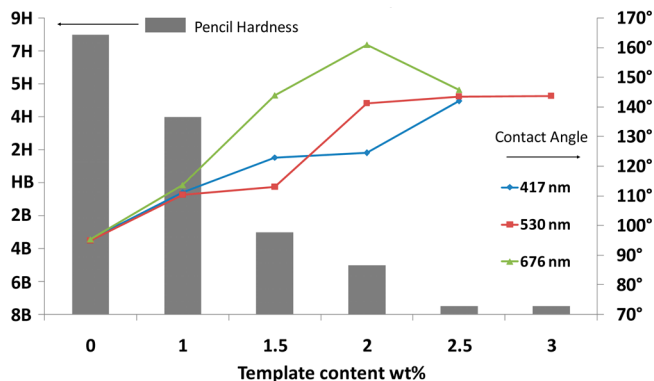

Figure 5. Plot of average pencil hardness (left *y*-axis) and contact angle (right *y*-axis) against increasing template content (wt %) for template sizes 417, 530, and 676 nm.

From Figure 5, there is a general trend of increasing contact angle with increasing template composition. Surface chemistry does not alter between films so this increase can be attributed to increasing surface roughness with increasing template content, evident in Figure 6. Crater films exhibit pencil hardness far exceeding 8B at lower template compositions. In addition to reasons discussed, the enhanced pencil hardness can be attributed to the surface geometry exhibiting improved resistance to lateral forces compared to structures in Figure 2. While more robust, the contact angle of these films however is relatively diminished (110−130°) which can be attributed to insufficient surface roughness. Upon higher template compositions there is a rapid trade-off between durability and contact angle. Evident in Figure 6c the films begin to resemble coral and exhibit large disconnections within the gel. The presence of these large voids introduces hierarchical roughness through combination of craters, spike fragments, and the voids themselves. The simultaneous decrease in pencil hardness is also attributed to this increasing level of porosity which is known to limit mechanical strength.[33−35] Durability was further investigated by tape adhesion (Supporting Information S1 and S2). It was expected that any layer removal should have minimal effects on water contact angles due to the crater morphology repeating itself throughout the bulk MTMS matrix which is intrinsically hydrophobic. Typically, changes in contact angle were minimal with subtle increases after tape adhesion tests (S1). There also exists one case where the contact angle dropped significantly. SEM images (Figure S2a and b) reveal

that increases in contact angle are likely due to minor fragments separating from the film. The voids generated introduce hierarchical nature to the surface roughness, akin to those which occur at increasing template concentrations illustrated in Figure 6a−c. Similarly, the case where contact angle was diminished, large portions of the film were removed (Figure S2c). Qualitatively it was observed with increasing porosity, additional film was removed therefore following a similar trend to pencil hardness. Pencil hardness and tape adhesion tests demonstrates the use of crater morphology to provide a robust framework for microroughness however also highlights diminishing returns toward improving contact angles based on single-scale templates. Future development toward the spray coating packing of multiscale templates may permit enhanced surface roughness at reduced bulk porosities. This would facilitate more robust hierarchical films and therefore allow enhanced contact angle while maintaining mechanical strength. While spray coating facilitates up-scaling, a current limitation to this procedure is a relatively high processing temperature (350 °C) to remove the polymer sphere templates. Future work to remove this processing hurdle could encompass the development of most sensitive templates toward thermal, pH,[36,37] or UV degradation.[38]

4. CONCLUSION

Polymer spheres prepared through emulsion synthesis were utilized as sacrificial templates within a siloxane matrix to yield films with craterlike surface roughness. Surface roughness was controlled through the template geometry, size, and concentration. The intrinsic hydrophobicity of the MTMS matrix provides enhanced longevity toward wear. The crater films prepared demonstrated robust microroughness with contact angles between 110 and 135°. Upon increased template concentration, the presence of spikes and large voids established hierarchical roughness and superhydrophobic contact angles. The increased porosity proved extremely detrimental to mechanical properties. Future work toward controlling multiscale template dispersion and decomposition in spray coated systems may facilitate the large scale practical application of robust superhydrophobic films.

■ ASSOCIATED CONTENT

Ⓢ Supporting Information

Contact angles (S1) and SEM images (S2) prior to and after tape-adhesion tests. This material is available free of charge via the Internet at http://pubs.acs.org.
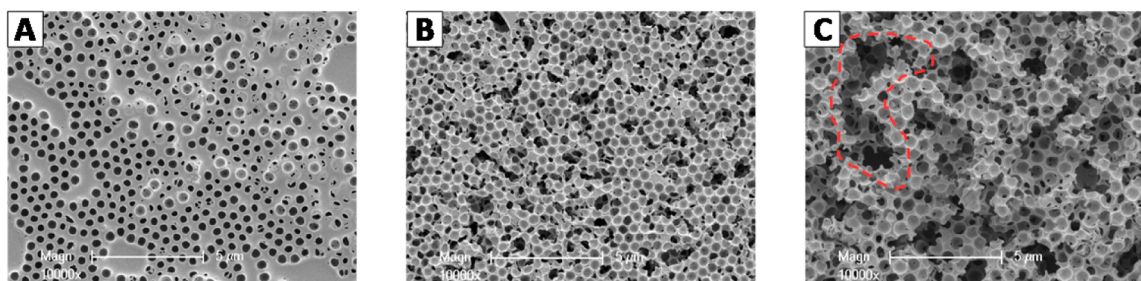

Figure 6. SEM micrographs A, B, and C illustrate crater films produced with 0.5, 1.5, and 3 template wt % (530 nm), respectively. Scale bars represent 5 *μ*m.

■ AUTHOR INFORMATION

Corresponding Author

*Tel.: +61 3 8344-6492. E-mail address: rnlamb@unimelb.edu.au.

Author Contributions

‡All authors contributed equally.

Notes

The authors declare no competing financial interest.

■ ACKNOWLEDGMENTS

■ REFERENCES

(1) Guo, Z.; Liu, W.; Su, B.-L. Superhydrophobic Surfaces: From Natural to Biomimetic to Functional. *J. Colloid Interface Sci.* **2011**, *353*, 335−355.

(2) David, Li.; Calama, C.; Mercedes, X.-M. What Do We Need for a Superhydrophobic Surface? A Review on the Recent Progress in the Preparation of Superhydrophobic Surfaces. *Chem. Soc. Rev.* **2007**, *36*, 1350−1368.

(3) Wu, A.-F.; Nakanishi, K.; Cho, K. L.; Lamb, R. Diatom Attachment Inhibition: Limiting Surface Accessibility through Air Entrapment. *Biointerphases* **2013**, *8*, 1−10.

(4) Cassie, A. B. D.; Baxter, S. Wettability of Porous Surfaces. *Trans. Faraday Soc.* **1944**, *40*, 546−550.

(5) Jones, A.; Lamb, R. N.; Zhang, H.; Uniserach Limited, AU. Hydrophobic Material. US Patent 6,743,467 B1, June 1, 2004.

(6) Verho, T.; Bower, C.; Andrew, P.; Franssila, S.; Ikkala, O.; Ras, R. H. A. Mechanically Durable Superhydrophobic Surfaces. *Adv. Mater.* **2011**, *23*, 673−678.

(7) Nakajima, A.; Abe, K.; Hashimoto, K.; Watanabe, T. Preparation of Hard Super-Hydrophobic Films with Visible Light Transmission. *Thin Solid Films* **2000**, *376*, 140−143.

(8) Nakajima, A.; Hashimoto, K.; Watanabe, T. Recent Studies on Super-Hydrophobic Films. *Monatsh. Chem.* **2001**, *132*, 31−41.

(9) Bhushan, B.; Nosonovsky, M. Scale Effects in Friction Using Strain Gradient Plasticity and Dislocation-Assisted Sliding (microslip). *Acta Mater.* **2003**, *51*, 4331−4345.

(10) Guo, Z. G.; Liang, J.; Fang, J.; Guo, B. G.; Liu, W. M. A Novel Approach to the Robust Ti6Al4V-Based Superhydrophobic Surface with Crater-Like Structure. *Adv. Eng. Mater.* **2007**, *9*, 316−321.

(11) Yanagisawa, T.; Nakajima, A.; Sakai, M.; Kameshima, Y.; Okada, K. Preparation and Abrasion Resistance of Transparent Super-Hydrophobic Coating by Combining Crater-Like Silica Films with Acicular Boehmite Powder. *Mater. Sci. Eng., B* **2009**, *161*, 36−39.

(12) Han, K. D.; Leo, C. P.; Chai, S. P. Fabrication and Characterization of Superhydrophobic Surface by Using Water Vapor Impingement Method. *Appl. Surf. Sci.* **2012**, *258*, 6739−6744.

(13) Yabu, H.; Shimomura, M. Single-Step Fabrication of Transparent Superhydrophobic Porous Polymer Films. *Chem. Mater.* **2005**, *17*, 5231−5234.

(14) Zhang, J.; Chen, Z.; Wang, Z.; Zhang, W.; Ming, N. Preparation of Monodisperse Polystyrene Spheres in Aqueous Alcohol System. *Mater. Lett.* **2003**, *57*, 4466−4470.

(15) Anderson, C. D.; Sudol, E. D.; El-Aasser, M. S. 50 Nm Polystyrene Particles via Miniemulsion Polymerization. *Macromolecules* **2001**, *35*, 574−576.

(16) *Standard Test Method for Film Hardness by Pencil Test*; , Standard D3363, ASTM International: West Conshohocken, PA, 2011; DOI: 10.1520/D3363-05R11E02.

(17) Velev, O. D.; Kaler, E. W. Structured Porous Materials via Colloidal Crystal Templating: From Inorganic Oxides to Metals. *Adv. Mater.* **2000**, *12*, 531−534.

(18) Ming, W.; Wu, D.; van Benthem, R.; de With, G. Super-hydrophobic Films from Raspberry-Like Particles. *Nano Lett.* **2005**, *5*, 2298−2301.

(19) Bayer, I. S.; Brown, A.; Steele, A.; Loth, E. Transforming Anaerobic Adhesives into Highly Durable and Abrasion Resistant Superhydrophobic Organoclay Nanocomposite Films: a New Hybrid Spray Adhesive for Tough Superhydrophobicity. *Appl. Phys. Express* **2009**, *2*, 5003.

(20) Zhang, H.; Lamb, R.; Jones, A.; Unisearch Limited, AU. Durable Superhydrophobic Coating. US Patent 2,007,009,657 A1, April 8, 2004.

(21) Takadoum, J. *Nanomaterials and Surface Engineering*; ISTEWiley, London, UK, Hoboken, NJ: ISTEWiley, 2010.

(22) Walter, R.; Rong, M.; Zhang, M.; Zheng, Y.; Zeng, H.; Friedrich, K. Structure−property Relationships of Irradiation Grafted Nano-Inorganic Particle Filled Polypropylene Composites. *Polymer* **2001**, *42*, 167−183.

(23) Paul, D. R.; Robeson, L. M. Polymer Nanotechnology: Nanocomposites. *Polymer* **2008**, *49*, 3187−3204.

(24) Iler, R. K. *The Chemistry of Silica: Solubility, Polymerization, Colloid and Surface Properties, and Biochemistry*; Wiley: New York, 1979.

(25) Stein, A. Sphere Templating Methods for Periodic Porous Solids. *Microporous Mesoporous Mater.* **2001**, *44−45*, 227−239.

(26) Venkateswara Rao, A.; Bhagat, S. D.; Hirashima, H.; Pajonk, G. M. Synthesis of Flexible Silica Aerogels Using Methyltrimethoxysilane (MTMS) Precursor. *J. Colloid Interface Sci.* **2006**, *300*, 279−285.

(27) Venkateswara Rao, A.; Kalesh, R. R. Comparative Studies of the Physical and Hydrophobic Properties of TEOS Based Silica Aerogels Using Different Co-Precursors. *Sci. Technol. Adv. Mater.* **2003**, *4*, 509−515.

(28) Nadargi, D. Y.; Rao, A. V. Methyltriethoxysilane: New Precursor for Synthesizing Silica Aerogels. *J. Alloys Compd.* **2009**, *467*, 397−404.

(29) Raman, N. K.; Anderson, M. T.; Brinker, C. J. Template-Based Approaches to the Preparation of Amorphous, Nanoporous Silicas. *Chem. Mater.* **1996**, *8*, 1682−1701.

(30) Kitaev, V.; Ozin, G. A. Self-Assembled Surface Patterns of Binary Colloidal Crystals. *Adv. Mater.* **2003**, *15*, 75−78.

(31) Cui, L.; Zhang, Y.; Wang, J.; Ren, Y.; Song, Y.; Jiang, L. Ultra-Fast Fabrication of Colloidal Photonic Crystals by Spray Coating. *Macromol. Rapid Commun.* **2009**, *30*, 598−603.

(32) Cho, K. L.; Liaw, I. I.; Wu, A. H.-F.; Lamb, R. N. Influence of Roughness on a Transparent Superhydrophobic Coating. *J. Phys. Chem. C* **2010**, *114*, 11228−11233.

(33) Rice, R. W. Comparison of Physical Property Porosity Behaviour with Minimum Solid Area Models. *J. Mater. Sci.* **1996**, *31*, 1509−1528.

(34) Spriggs, R. M. Expression for Effect of Porosity on Elastic Modulus of Polycrystalline Refractory Materials, Particularly Aluminum Oxide. *J. Am. Ceram. Soc.* **1961**, *44*, 628−629.

(35) Gibson, L. J.; Ashby, M. F. *Cellular Solids: Structure and Properties*; Cambridge University Press, 1999.

(36) Simovich, T.; Wu, A. H.; Lamb, R. N. Energy Efficient One-Pot Synthesis of Durable Superhydrophobic Coating through Nylon Micro-Rods. *Appl. Surf. Sci.* **2014**, *295*, 203−206.

(37) Bruggeman, J. P.; de Bruin, B.-J.; Bettinger, C. J.; Langer, R. Biodegradable Poly(polyol Sebacate) Polymers. *Biomaterials* **2008**, *29*, 4726−4735.

(38) Kumar, A. P.; Depan, D.; Singh Tomer, N.; Singh, R. P. Nanoscale Particles for Polymer Degradation and stabilization—Trends and Future Perspectives. *Prog. Polym. Sci.* **2009**, *34*, 479−515.